

Qingqing GAI, Qiuye LIU, Wenyong LI, Xiwen HE, Langxing CHEN, Yukui ZHANG

Preparation of bovine hemoglobin-imprinted polymer beads via the photografting surface-modified method

© Higher Education Press and Springer-Verlag 2008

Abstract Molecularly imprinted polymers (MIPs), based on photografting surface-modified polystyrene beads as matrices, were prepared with acrylamide as the functional monomer, bovine hemoglobin as the template molecule and *N, N'*-methylene bisacrylamide as the crosslinker in a phosphate buffer. The results of IR, scanning electron microscope (SEM) and elemental analyses demonstrated the formation of a grafting polymer layer on the polystyrene-bead surface. Subsequent removal of the template left behind cavities on the surface of the polymer matrix with a shape and an arrangement of functional groups having complementary binding sites with the original template molecule. The adsorption studies showed that the imprinted polymers have a good adsorption capacity and specific recognition for bovine hemoglobin as the template molecule. Our results demonstrated that the polymer prepared via the photografting surface-modified method exhibited better selectivity for the template. Attempts to employ the new method in molecular imprinting techniques may introduce new applications for MIPs and facilitate probable protein separation and purification.

Keywords molecular imprinting, molecular recognition, bovine haemoglobin, iniferter, photografting

Translated from *Chemical Journal of Chinese Universities*, 2008, 29(1): 64–70

Qingqing GAI, Qiuye LIU, Wenyong LI, Xiwen HE (✉), Langxing CHEN, Yukui ZHANG

Department of Chemistry, Nankai University, Tianjin 300071, China

Yukui ZHANG (✉)

Dalian Institute of Chemical Physics, Chinese Academy of Sciences, Dalian 116011, China

E-mail: ykzhang@dicp.ac.cn

Qingqing GAI

Changzhi Medical College, Changzhi 046000, China

1 Introduction

Molecular imprinting is a promising technique for preparing host compounds for molecule-specific recognition sites in robust network polymers using the polymerization of cross-linking agents and functional monomers in the presence of the template. The resulting polymers are chemically and mechanically stable molecularly imprinted polymers (MIPs) [1–3]. After template removal, MIPs afford complementary recognition sites which are able to selectively recognize the template during subsequent rebinding procedures. Usually, only low molecular weight compounds such as amino acid derivatives, and certain drugs and pesticides [4–12] are used as imprinted molecules, while biomacromolecules such as proteins are seldom used [13,14]. The limitations include their large molecular sizes, which makes it difficult for macromolecules to slip in and out of a polymer network, and the complexity of the protein structure and the variety of their sequences, which make well-defined recognition sites hard to produce. However, some success in imprinting biomacromolecules, such as proteins, has been mainly achieved through different strategies [15–19].

At present, protein imprinting can be broadly classified into three ways: entrapment [20], the “epitope” approach [21] and microsphere surface imprinting [22]. Although the method of protein entrapment is simple, the post-treatment process is troublesome and time-consuming. Further, the morphology of polymer particles gets worse. Another difficulty is that large molecules close to internal imprinted sites embed in the polymer with serious space steric effects. The “epitope” approach is very complicated, and needs to identify the protein structure and assay epitopes, but some target proteins have no epitopes with definite polypeptide length. Therefore, the use of the “epitope” approach is restricted. The approach using microbead surface imprinting prepares molecularly imprinted polymers by decorating the surface of the particles. At first the proteins and the functional monomer pre-assemble on the surface of microspheres, and then the polymer layer with the proteins partly embedded on

the surface of the microspheres is formed. After removal of the proteins, many cavities are left in the polymer layer, the shape and functions of which are complementary to the surface of the template protein. The polymers prepared using surface imprinting are uniformly spherical particles and have mechanical stability. As a result of the recognition sites on the surface of the microspheres, the protein template can then quickly adjoin to the sites. This can greatly reduce the non-specific absorption effect on selectivity and the embedding phenomenon [23,24]. It is a promising imprinting for macromolecules.

Initiator transfer agent terminator (iniferter) is a particular free radical terminator which has the effects of initiation, transformation and termination during the whole process of polymerization. It is decomposed into a living and inert radical under ultraviolet radiation. The former process involves attaching to the surfaces of supports, which may originate polymerization of monomers, and the latter is concerned with the free radical terminating reaction and chain transferring reaction in medium [27]. Therefore, in a way, gelation can be avoided. Ruckert [28] et al. reported that molecularly imprinted composites prepared from iniferter-modified supports exhibited pronounced imprinting effects and were capable of separating the template D- L-phenylalanine anilide from its enantiomers.

In this work, MIPs based on photografting surface-modified polystyrene beads as matrices were prepared with acrylamide as the functional monomer, bovine hemoglobin as the template molecule, *N, N'*-methylene bisacrylamide as the crosslinker and sodium diethyldithiocarbamate trihydrate as the iniferter in a phosphate buffer. The results of IR, SEM and elemental analyses demonstrate the formation of a grafting polymer layer on the polystyrene-bead surface. Further, adsorption studies show that the imprinted polymers created *via* the photografting surface-modified method exhibited better adsorption capacities and specific recognition for the template molecule. Based on these, our attempt to employ the new method in molecular imprinting techniques may introduce new applications for MIPs, and facilitate probable protein separation and purification.

2 Experiments

2.1 Materials and reagents

Bovine hemoglobin (BHb), bovine serum albumin (BSA), lysozyme (LYZ) and ovalbumin (OB) were purchased from Lanji Sci-Technology Company (Shanghai, China) and the protein solutions were prepared using 0.01 M sodium dihydrogen phosphate buffer. Macropore polystyrene beads (MPC) were obtained from Tianjin Nankai Synthesized Science and Technique Ltd.

Sodium diethyldithiocarbamate trihydrate (NaDEDTC) was purchased from the Tianjin Guangfu Fine Chemicals Institute. Acrylamide (AA) and sodium dodecyl sulfate (SDS) were purchased from the Tianjin Yongda Chemical Reagent Factory. *N, N'*-methylenebisacrylamide (MBA) was purchased from the Tianjin Chemical Reagent Institute. Acetic acid was obtained from the Tianjin No.6 Chemical Reagent Factory. Other chemicals were all analytical grade and used as received without further purification. Deionized water was used throughout.

C and H elements were measured by Elementar Vario EL meter. UV-vis and IR spectra were recorded by means of a Shimadzu model UV-2450 and a Bruker model EQYINOX-55 spectrophotometer. A vibrator and a centrifuge were employed for obtaining analytes of the proteins. The surface configuration of polystyrene-beads was observed by EFI Quanta 200 SEM.

2.2 Preparation of BHb-imprinted Polymers

The preparation process of BHb-imprinted polymers using optimized conditions are summarized as follows: the MPC beads (4 g) were suspended in ethanol (20 mL) and 12 mL of 10% NaDEDTC dissolved in ethanol was added dropwise. Subsequently, the suspension was stirred at 50°C overnight. The particles were washed with ethanol and acetone three times, and then dried at 40°C under vacuum overnight. This resulted in MPC-grafted beads with the surfaces of the MPCs modified by the iniferter.

BHb (200 mg), acrylamide (2.851 g), and *N, N'*-methylenebisacrylamide (153.5 mg) were dissolved in 50 mL of 0.01 mol/L phosphate buffer solution (pH 5.4) in a 100 mL conical flask and prepolymerized for 12 h in the vibrator. Then 2 g of MPC-grafted beads were added into the solution, deoxygenated by sonication for 10 min and then sealed. The polymerization occurred overnight at room temperature under ultraviolet radiation for 12 h. The BHb-imprinted polymers (BHb-MIPs) were synthesized.

In the vibrator, BHb-MIPs were washed with 10% (*V/V*) acetic acid containing 10% (*W/V*) SDS solution to elute the template BHb, and then with 0.01 M phosphate buffer solution (pH 5.4) time and again to remove other unreactive reagents. Then the washed BHb-MIPs were dried in vacuum until their masses became invariable. The concentration of BHb in the elution solution was monitored by a UV-vis spectrophotometer at 405 nm until the value of absorbance received was less than 5% of the original.

The non-imprinted polymers (NIP) were prepared in the same manner in the absence of BHb.

2.3 Adsorption experiments of BHb-MIP

To investigate the adsorption dynamics of the imprinted polymers, 10.0 mg of BHb-MIPs was placed in a tube and

mixed with 5 mL of 0.6 mg/mL BHb solution (pH 5.4). The tube was sealed and oscillated in an oscillator at 25°C. Following the incubation period, the MIPs were settled by centrifugation at 3000 rpm for 15 min at specific time intervals and the sample was withdrawn from the supernatant. Then the concentration of BHb in the solution was determined by spectrophotometry at 405 nm. To determine the static equilibrium adsorption capacity, 10.0 mg of BHb-MIP was placed in a tube and mixed with 5 mL of a known concentration of BHb solution (pH 5.4). The tube was sealed and oscillated in an oscillator at 25°C for 3 h. The other processes are as described above.

Meanwhile, competitive adsorption experiments on BHb were done on BHb-MIPs. BSA, LYZ and OB were chosen as the competitive proteins. A series of 10.0 mg BHb-MIPs were placed in tubes and respectively added into 5 mL mixed solutions of the template BHb and a competitive protein (pH 5.4), with a fixed concentration of BHb (0.2 mg/mL) and increasing concentrations of each competitive protein (0.1–1.0 mg/mL) in the vibrator for 3 h. The other processes are as above. The concentrations of BHb and the competitive proteins in solution were determined and were calculated by the value of absorbance at 405 nm and 278 nm, respectively.

The adsorption capacity (Q) was calculated based on the change in the protein concentration in the solution before and after adsorption, the volume of the aqueous solution, and the weight of the polymers. The experimental data is presented as the adsorption capacity per unit mass (g) of polymers, and Q is calculated according to

$$Q = (\rho_0 - \rho_t)V/m,$$

Where ρ_0 is the initial protein concentration (mg/mL), ρ_t is the protein concentration (mg/mL) of different times, V is the volume of protein solution (mL), and m is the mass of the polymers.

3 Results and discussion

3.1 Preparation process of the BHb-MIP beads via the photografting surface-modified method

Polystyrene beads are used as matrices because of their adequate mechanical intensity and simple preparation steps, while surfaces with silica gels as matrices need to be dealt with by silanisation, endcapping and so on. Therefore, polystyrene beads are more fit for studying life sciences and environmental sciences. The process of preparation is shown in Fig. 1.

3.2 Surface morphology of polymers beads

3.2.1 SEM microphotographs

The monolithic structure and the change of surface configuration of polymer beads before and after grafting were observed by SEM. The SEM microphotographs in Figs. 2 (A) and (B) indicate that the surfaces of the ungrafted macro polystyrene (MPC) beads are slick and their sizes are regular, ranging from 38 to 50 μm . Fig. 2(C) presents the surface of MPC-grafted beads with iniferter. The figure distinctly shows that the surface is uneven, and in some parts totally absent and alveolate. As seen in the schematic view of Fig. 2 (D), BHb-MIPs beads, after removing template BHb, have rough surfaces, an inhomogeneous thickness, and exhibit a peculiar folded structure.

3.2.2 IR spectra

Figures 3 (a), (b) and (c) represent the IR spectra of MPC beads, MPC-grafted beads and BHb-MIPs beads, respectively. From Fig. 3 (b), we can see that a 1415 cm^{-1} strong absorption peak and a 1354 cm^{-1} weak absorption peak are

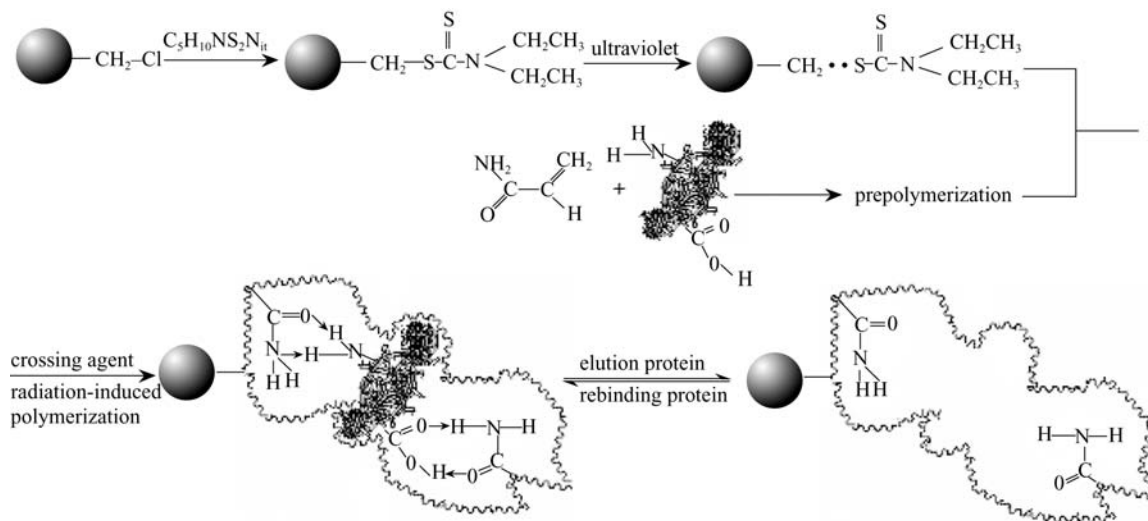


Fig. 1 Procedure for preparing the protein-imprinted polymer

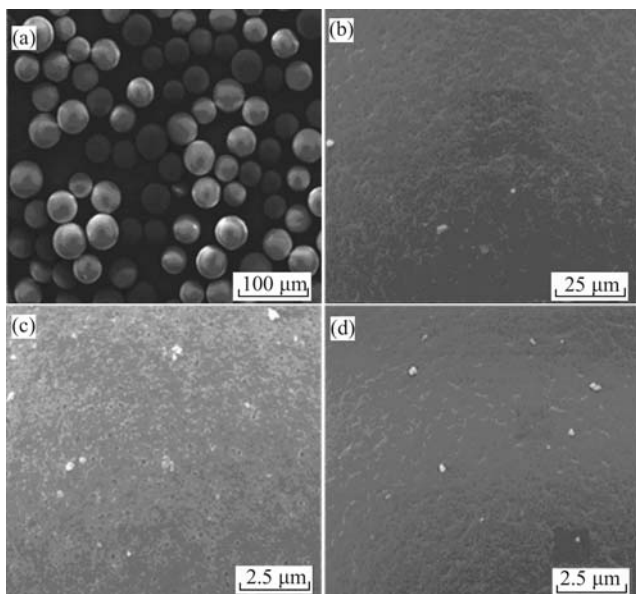


Fig. 2 SEM microphotographs of (A) and (B) MPC beads; (C) MPC grafted beads; (D) MIP beads

deformation vibrations of saturated C–H bonds of NaDEDTC, and that a 1208 cm^{-1} absorption peak reflects stretching vibrations of C=S bonds after MPC beads are grafted by the iniferter. The results denote that the iniferter was successfully grafted onto the MPC beads. In Fig. 3 (c) the 1630 cm^{-1} absorption peak shows the vibration of the C=O bond of acrylamide and *N, N'*-methylene bisacrylamide. It demonstrates that the functional monomer and the crosslinker were included in the BHB-MIPs beads.

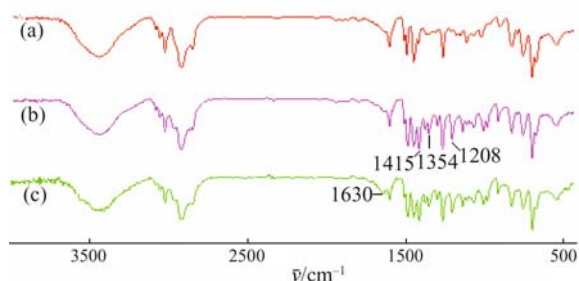


Fig. 3 IR spectra of (a) MPC beads; (b) MPC grafted beads; (c) MIP beads

3.2.3 Elemental analysis

From the elemental analysis datum on MPC beads, MPC-grafted beads and BHB-MIPs beads, we see that the N content is 0% and the C content is 80.11% in MPC beads, and that the content of the corresponding N and C are 1.77% and 74.35%, respectively, in the MPC-grafted beads. In other words, the iniferter modified into MPC beads makes the N content rise and the C content decline. However, the addition of acrylamide as the functional monomer and *N, N'*-methylene bisacrylamide as the

crosslinker into the polymerization makes the content of N decline and the content of C rise to a certain extent.

The results of IR, scanning electron microscope (SEM) and elemental analyses illuminate the formation of a grafting polymer layer on the MPC bead surface utilizing an iniferter.

3.3 Adsorption characteristics and selective recognition of MIP

3.3.1 Adsorption dynamics of BHB on MIP

Adsorption capacity-adsorption time curves of adsorption experiments on MIP-BHB to template BHB are shown in Fig. 4. The adsorption capacity of BHB in solution was calculated by the decrease in concentration of BHB. The adsorption capacity had a rapid increase for the first 60 min, and then slowed down in the later stages until reaching adsorption equilibrium at 180 min. It is obvious that the adsorption process has two stages. In the beginning, the adsorption capacity increases rapidly because of BHB adsorbing onto the surface of MIP-BHB; after that, the adsorption rate slows down due to the difficulty in penetrating into the MIP-BHB. Adsorption equilibrium is obtained probably because both BHB and the cavities in the structure of the imprinted polymer have a high degree of coordination and memory effect. The binding cavities created during the imprinting process are complementary in shape and function to the template molecule. The greatest adsorption capacity of BHB on MIP-BHB is 63.5 mg/g . Though the aqueous as polar solvent has some effect on the formation of hydrogen bonds between the template and MIP, many interactional imprinting sites are created in MIP by virtue of its large protein size. So the effect of the aqueous is weak in the rebinding of the protein. The peptide bonds of the protein could form multiple-point hydrogen bonds with the AM

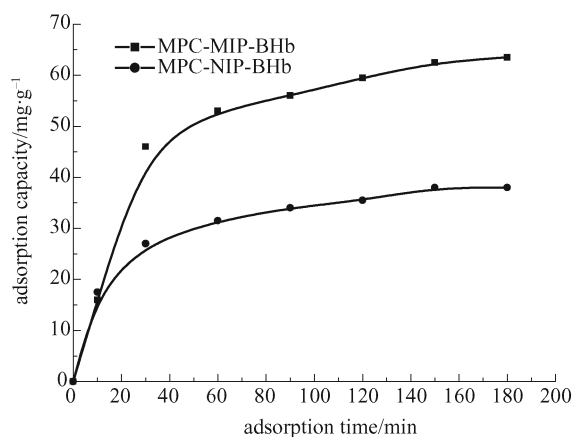


Fig. 4 Adsorption dynamic curve of template BHB on MIP and NIP beads

Initial BHB concentration: 0.6 mg/mL ; sample quantity: 10.0 mg ; pH: 5.4 in PBS; temperature: 25°C

even in polar solutions, and the multiple-point hydrogen bond interactions make them form strong interaction forces [29]. MIPs have more imprinting sites and generate higher adsorption capacity compared to template proteins. We can see that imprinting NIP onto BHB has the same adsorption trend as MIP. The adsorption capacity of NIP onto BHB increases as time progresses, and then adsorption achieves equilibrium as seen in Fig. 4. The largest adsorption capacity of BHB on NIP is 38.0 mg/g. This may be non-specific adsorption caused by hydrophobic interactions, van der Waals forces, and the interaction of hydrogen bonds between BHB and surface groups of NIP due to BHB spreading into the NIP.

3.3.2 Adsorption isotherm

Figure 5 gives the adsorption equilibrium isotherm for the adsorption of BHB onto BHB-MIP. The adsorption capacity increases with the concentration increase of BHB. When the initial concentration of BHB is below 0.4 mg/mL, the adsorption capacity will increase rapidly. When the initial concentration of BHB is higher than 0.4 mg/mL, adsorption curves become relatively smooth. When it reached roughly 0.6 mg/mL, adsorption reached saturation, which showed that the active bonding cavities on BHB-MIP reached saturation. The greatest adsorption capacity of BHB on MIP and NIP is 63.5 mg/g and 38.0 mg/g, respectively. The values are consistent with those in Fig. 4. Figure 5 shows that BHB-MIP exhibited a higher adsorption capacity and better selectivity of BHB compared to NIP. As BHB-MIP possesses the three-dimensional cavities formed in the pre-polymerization stage as well as binding sites created after removal of BHB, a major factor in the adsorption process is molecularly specific recognition. The imprinting cavities and binding sites in MIP adsorb a large number of BHB, so the imprinting process can obtain higher adsorption capacities.

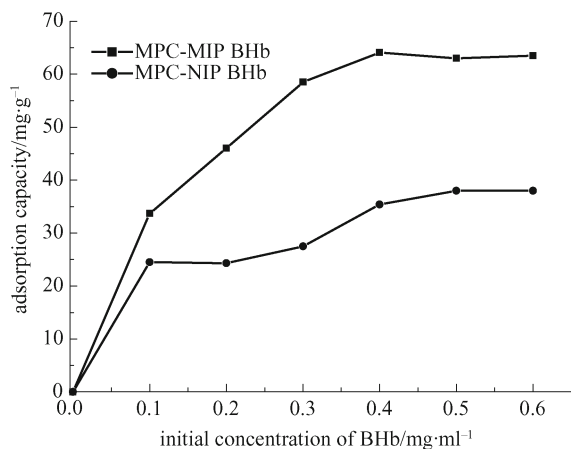


Fig. 5 Adsorption isotherms of BHB on MIP and NIP beads. Sample quantity: 10.0 mg; pH: 5.4 in PBS; temperature: 25°C; adsorption time: 3 h.

Usually, the recognition selectivity of the imprinted polymer can be evaluated by using the imprinted factor (α), where α is defined as follows:

$$\alpha = Q_{\text{MIP}} / Q_{\text{NIP}} \quad (1)$$

Q_{MIP} and Q_{NIP} are the adsorption capacities of the protein in the imprinted polymers and the non-imprinted polymers, respectively. The value of α is 1.67.

The adsorption behaviors of BHB-MIPs can be further described by the Langmuir absorption equation as

$$\rho_e / Q = \rho_e / Q_{\text{max}} + 1 / (K Q_{\text{max}}) \quad (2)$$

where ρ_e is the equilibrium concentration of BHB (mg/mL), Q_{max} is the theoretical maximum adsorption capacity (mg/g), K is the Langmuir adsorption equilibrium constant (mL/mg), and r_L is the correlation coefficient of the isotherm. A linearized plot of ρ_e / Q versus ρ_e (Fig. 6) gives the adsorption curve. The Q_{max} and K values can be calculated from the slope and the intercept of the Langmuir regression equation to be 71.39 mg/g and 19.98 mg/g of MIP, respectively. The Q_{max} and K values can be calculated to be 43.06 mg/g and 12.75 mg/g of NIP, respectively. It can be seen from the data that the Langmuir equation fits well for BHB adsorption on the MIP under the concentration range studied (correlation coefficient $r_L = 0.992$). According to the adsorption isotherm, the greatest absorption capacity and the Langmuir equilibrium constant of MIP are bigger than NIP, and the linear relationship of MIP is better than that of NIP ($r_L = 0.975$).

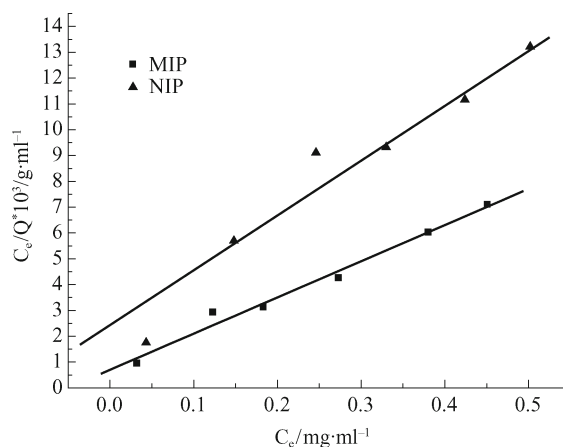


Fig. 6 Adsorption isotherm of BHB on MIP and NIP beads, linearized according to the Langmuir equation. c_e : the equilibrium concentration of BHB; sample quantity: 10.0 mg; pH: 5.4 in PBS; temperature: 25°C; adsorption time: 3 h.

3.3.3 Specific selectivity MIP

With the equilibrium adsorption method, the amounts of template protein BHB (68000) and competitive protein

BSA (66400), LYZ (13400) and OB (44200) on MIP and NIP can be determined, and the specific selectivity of MIP can be inspected. The specific approaches are as follows: four 10.0 mg MIPs are taken, and each of the MIPs is added to 0.2 mg/mL of BHb, BSA, LYZ and OB phosphate buffer solutions, respectively. Other experimental conditions are consistent with adsorption isotherm experiments. Figure 7 presents the adsorption capacities of template protein BHb and the three competitive proteins, BSA, LYZ, and OB, on MIP and NIP. The results showed that BHb on MIP has a higher adsorption capacity and those of the three competitive proteins are relatively low, which only approximate BHb on NIP. We can thus infer that physical adsorption plays an important role in the adsorption of competitive proteins, and that the molecular imprinting process did not have much effect on it. The results also show that the adsorption capacities of the non-template BSA, LYZ and OB are close to each other and are far smaller than the corresponding value of the template BHb. Under the same conditions, the adsorption capacities of the template and non-template on NIP are relatively small. MIP exhibits better selective recognition of BHb. It is clear that the microenvironment created during the imprinting process is based on shape selection and positioning of functional groups to recognize the BHb imprinting molecule.

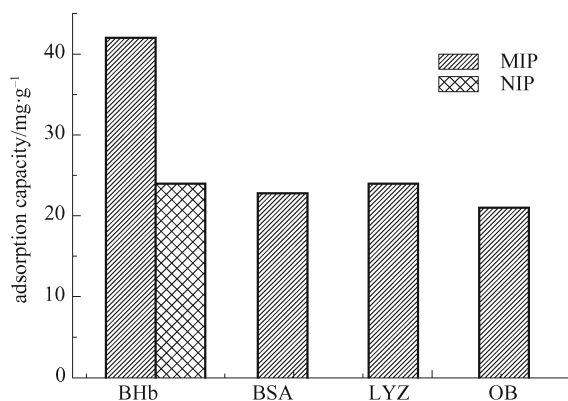


Fig. 7 Adsorption capacity of BHb-MIP and NIP for BHb, BSA, LYZ and OB, respectively

The initial concentrations of BHb, BSA, LYZ and OB were 0.2 mg/mL, respectively; sample quantity: 10.0 mg; pH: 5.4 in PBS; temperature: 25°C; adsorption time: 3 h

Though BHb and BSA are both global proteins and have approximately similar molecular weights, BHb is a tetrameric protein composed of pairs of two different polypeptides and has a biconcave shape, whereas BSA consists of one polypeptide and has an ellipsoidal shape [30]. Since the cavities formed on MIP are matched to the size of BHb, it is very difficult for the molecules having other dimensions to enter the cavities. The molecular weights of both LYZ and OB are less than BHb, so the

molecular sizes of LYZ and OB are smaller than BHb. Although LYZ and OB in the volume can easily enter into the cavities of MIP, it is hard to have a specific absorption for their structure, and the functional groups do not match. Thus, the absorption capacity of MIP to a non-template is correspondingly lower.

3.3.4 Competitive adsorption experiment

In the mixtures of template BHb and a competitive protein in phosphate buffer solution, the adsorption capacity of BHb on MIP was studied, with a fixed concentration of BHb (0.2 mg/mL) and an increasing concentration of BSA, LYZ and OB (0.1–1.0 mg/mL), respectively.

Figures 8 A–C show the competitive adsorptions of MIP and NIP for the imprinting molecule BHb, with the invariable concentrations of BHb and the continuous increase in the concentrations of BSA, LYZ and OB in the mixture of the two proteins. It can be seen from Fig. 7 and Fig. 8 that compared with single adsorption experiments, adsorption capacities of both MIP and NIP for BHb in the competitive adsorption experiments become smaller. Since the cavities and binding sites formed in MIP are matched to BHb, MIP is easily bound to BHb and exhibits specific adsorption for BHb in the mixed solution. However, although competitive proteins are not so predominant like the imprinting protein, they still have a little adsorption on MIP. So the adsorption capacity of BHb on MIP is lower in the competitive adsorption experiment than in the single adsorption experiment.

As observed in Fig. 8, the adsorption capacity of BHb on MIP has a little reference to the concentration of the competitive protein. It can not be rapidly decreased by increasing the concentration of competitive proteins. It is clear that the increase in the concentration of competitive proteins almost does not impact the adsorption capacity of BHb on MIP and NIP. In other words, the bonding capacity of BHb on MIP is almost unchanged with the increase in concentration of competitive proteins. From this we can see that MIP has higher specific selectivity for BHb. The multi-point hydrogen bonds and the shape complementarity formed by the imprinting process play a crucial role in selective recognition. The specific absorption related to molecular imprinting always has an important selectivity for the template protein. Therefore, we conclude that molecular imprinting exhibits a better specific selectivity for BHb at a lower concentration, and it is expected to assist in the enrichment of low abundance proteins.

Acknowledgements The project was supported by the National Basic Research Program of China (No. 2007cb914101), the National Natural Science Foundation (Grant No. 20675040) and the Natural Science Foundation of Tianjin (No. 06YFJMJC02800 and No. 07JCYBJC00500).

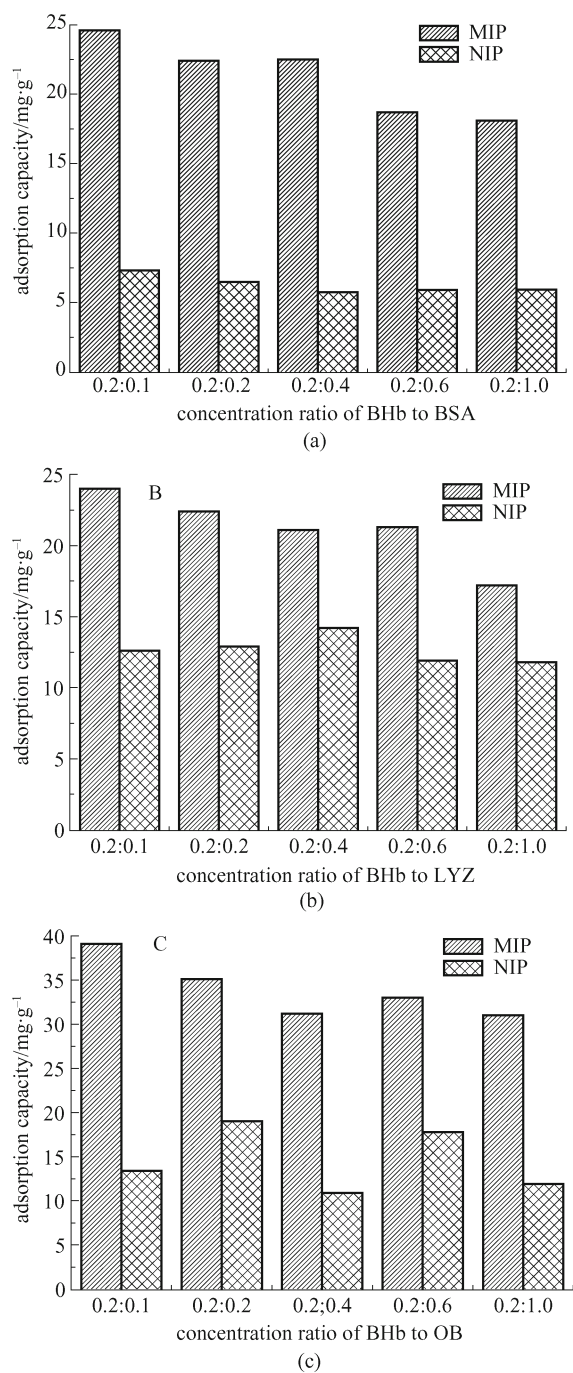


Fig. 8 Competitive adsorption of the template protein BHB in respect to competing proteins. Competitive adsorption experiments were done on MIP and NIP beads at pH 5.4 for 3 h, with a fixed concentration of BHB (0.2 mg/mL) and increasing concentrations of competing proteins (0.1–1.0 mg/mL)

References

1. Wulff G. Molecular imprinting in cross-linked materials with the aid of molecular templates—a way towards artificial antibodies. *Angew Chem Int Ed Engl*, 1995, 34: 1812–1832
2. Mosbach K. Molecular imprinting. *Trends Biochem Sci*, 1994, 19: 9–14

3. Haupt K, Mosbach K. Molecularly imprinted polymers and their use biomimetic sensors. *Chem Rev*, 2000, 100: 2495–2504
4. Hu S G, Li L, He X W. Comparison of trimethoprim molecularly imprinted polymers in bulk and in sphere as the sorbent for solid-phase extraction and extraction of trimethoprim from human urine and pharmaceutical tablet and their determination by high-performance liquid chromatography. *Anal Chim Acta*, 2005, 537: 215–222
5. Hu S G, Li L, He X W. Solid-phase extraction of esculetin from the ash bark of Chinese traditional medicine by using molecularly imprinted polymers. *J Chromatogr A*, 2005, 1062: 31–37
6. Guo H S, He X W, Li Y J. Imprinted polymeric film-based sensor for the detection of dopamine using cyclic voltammetry. *Chinese J of Chem*, 2003, 21: 1624–1629
7. Rong F, Feng X G, Li P, Yuan C W, Fu D G. Preparation of imprinted polymer microbeads using iniferter photografting surface-modified method *Chinese science Bulletin*, 2006, 51(13): 1504–1508
8. Anderson L, Sellergren B, Mosbach K. Imprinting of amino acid derivatives in macroporous polymers. *Tetrahedron Lett*, 1984, 25: 5211–5214
9. Yoshida M, Hatate Y, Uezu K, Goto M, Furusaki S. Chiral-recognition polymer prepared by surface molecular imprinting technique. *Colloids Surfaces A*, 2000, 169: 259–269
10. Vlatakis G, Andersson L I, Mosbach K. Drug assay using antibody mimics made by molecular imprinting. *Nature*, 1993, 361: 645–647
11. Quaglia M, Chenon K, Hall A J. Target analogue imprinted polymers with affinity for folic acid and related compounds. *J Am Chem Soc*, 2001, 123: 2146–2154
12. Fisher L, Muller R, Ekberg B. Direct enantioseparatory phase prepared by molecular imprinting. *J Am Chem Soc*, 1991, 113: 9358–9360
13. Burow M, Minoura N. Molecular imprinting: synthesis of polymer particles with antibody-like binding characteristics for glucose oxidase. *Biochem Biophys Res Commun*, 1986, 227: 419–422
14. Shi H, Tsai W B, Garrison M D, Ferrari S, Ratner B D. Template-imprinted nanostructured surfaces for protein recognition. *Nature*, 1999, 398: 593–597
15. Yang H H, Zhang S Q, Yang W, Chen X L, Zhuang Z X, Xu J G, Wang X R. Molecularly imprinted sol-gel nanotubes membrane for biochemical Separations. *J Am Chem Soc*, 2004, 126: 4054–4055
16. Pang X S, Cheng G X, Lu S L, Tang E J. Synthesis of polyacrylamide gel beads with electrostatic functional groups for the molecular imprinting of bovine serum albumin. *Anal Bioanal Chem*, 2006, 384: 225–230
17. Mi H F, Guo M J, Zhao Z, Fan Y G, Wang C H, Shi L Q, Xia J J, Long Y. Protein-imprinted polymer with immobilized assistant recognition polymer chains. *Biomaterials*, 2006, 27: 4381–4387
18. Lin T Y, Hu C H, Chou T C. Determination of albumin concentration by MIP-QCM sensor. *Biosensors and Bioelectronics*, 2004, 20: 75–81
19. Bossi A, Bonini F, Turner A P F, Piletsky S A. Molecularly imprinted polymers for the recognition of proteins: The state of the art. *Biosensors and Bioelectronics*, 2007, 22: 1131–1137
20. Venton D L, Gudipati E. Influence of protein on polysiloxane polymer formation—Evidence for induction of complementary protein-polymer interactions. *Biochim Biophys Acta*, 1995, 1250: 126–136

21. Rachkov A, Minoura N. Towards molecularly imprinted polymers selective to peptides and proteins. The epitope approach. *Biochim Biophys Acta*, 2001, 1544: 255–266
22. Kempe M, Mosbach K. Separation of amino acids, peptides and proteins on molecularly imprinted stationary phases. *J Chromatogr A*, 1995, 691: 317–323
23. Nicholls I A, Rosengren J P. *Bioseparation*, 2002, 10: 301–305
24. Zhang W Y, Li X, Zhu L L. Advances in preparation of surface molecularly imprinted materials. *Modern Chemical Industry*, 2005, 12: 20–23
25. Qin S H, Qiu K Y. Living radical polymerization and copolymerization of vinyl monomers initiated with novel iniferters. *Acta Polymerica Sinica*, 2002, 2: 127–136
26. Chen, Wang G J. Preparation of block and graft copolymer with iniferters. *Polymer Bulletin*, 2003, 4: 79–84
27. Tamayo F G, Titirici M M, Esteban A M. Synthesis and evaluation of new propazine-imprinted polymer formats for use as stationary phases in liquid chromatography. *Anal Chim Acta*, 2005, 542: 38–46
28. Rukert B, Hall A, Sellergren B. Molecularly imprinted composite materials via iniferter-modified supports. *J Mater Chem*, 2002, 12: 2275–2280
29. Pang X S, Cheng G X, Li R S, Lu S L, Zhang Y H. Bovine serum albumin-imprinted polyacrylamide gel beads prepared via inverse-phase seed suspension polymerization. *Anal Chim Acta*, 2005, 550: 13–17
30. Guo T Y, Xia Y Q, Hao G J, Song M D, Zhang B H. Adsorptive separation of hemoglobin by molecularly imprinted chitosan beads. *Biomaterials*, 2004, 25: 5905–5912